The Otish Basin: Basin Evolution and Formation of the Camie River Uranium Deposit, Quebec

Dejan Milidragovic[1], Marion Lesbros-Piat-Desvial[1], Julia J. King[1], Georges Beaudoin[1], Mike A. Hamilton[2], and Robert A. Creaser[3]

1. Département de géologie et de génie géologique, Université Laval, 1065 avenue de la Médecine, Québec, Québec, G1V 0A6

2. Jack Satterly Geochronology Lab, Department of Earth Sciences, University of Toronto, 22 Russell Street, Toronto, Ontario, M5S 3B1

3. Department of Earth and Atmospheric Sciences, 1-26 Earth Sciences Building, University of Alberta, Edmonton, Alberta, T6G 2E3

Abstract

The Otish Basin of central Québec hosts over thirty uranium prospects, including the Camie River prospect that is located near the unconformable contact between the graphite-bearing, metamorphic basement of Archean age and the overlying basinal sedimentary rocks of the Otish Supergroup. The maximum age of the basin, constrained by the age of the unconformably-underlying Mistassini dyke swarm, is 2515 ± 3 Ma. Following the deposition of the Otish Supergroup, the basin was intruded by the Otish Gabbros, a suite of olivine-tholeiitic dykes and sills of near-liquid compositions (Group 1) and cumulate rocks (Group 2). Uranium-lead zircon ages from the Otish Gabbros indicate the minimum age of the Otish Basin is ca. 2.17 Ga. The Otish Basin was also intruded by the Matoush dyke, interpreted to be younger than the Otish Gabbros. The least altered samples of the Matoush dyke have mineralogy and trace element systematics, such as highly fractionated REE patterns, similar to lamprophyric rocks and are distinct from the tholeiitic to weakly trace element-enriched Otish Gabbros. This, therefore, indicates that the Otish Basin was affected by at least two igneous events.

The uranium mineralization formed after the peak diagenetic alteration of the Otish Supergroup. During peak diagenetic conditions, early albitic sandstone cement was largely replaced by K-feldspar. The feldspathic cement was subsequently partially replaced by a green muscovite alteration. The increase in Na_2O concentrations of the feldpsathic-cemented sandstones towards the base of the sedimentary sequence is noteworthy. Uraninite and brannerite are the principal uranium minerals at the Camie River prospect. Molybdenite grains, intergrown with uraninite, yield a Re-Os model age of 1724 ± 4.9 Ma that is indistinguishable from the previously published uraninite ages. The age of mineralization is significantly younger than the age of the Otish Gabbros, indicating that the uranium mineralization postdates sedimentation by ≥450 m.y. The overlapping Sm-Nd isotopic ages from Otish Gabbros suggest the main uranium mineralization was locally accompanied by resetting of the Sm-Nd system and LREE mobility in the gabbros. The age of mineralization in the Otish Basin is similar to the age of polymetallic mineralization of the Huronian Supergroup, suggesting the ca. 1.7 Ga hydrothermal activity may have been a regional phenomenon affecting the southern Superior Province.

Introduction

The Paleoproterozoic Otish Basin of central Québec hosts over thirty uranium prospects (Gatzweiler, 1987), many of which remain poorly understood and underexplored. Globally, Proterozoic sedimentary basins host several world-class uranium deposits (e.g. Ranger and Jabiluka deposits in MacArthur Basin, Australia and Cigar Lake and McArthur River deposits in Athabasca Basin, Canada), providing clear impetus for a better understanding of the style and mechanisms of uranium-enrichment in the Otish Basin. This report primarily examines the Camie River prospect (7.83 wt. % U_3O_8 over 1 m, Gatzweiler, 1987; 1 wt. % U_3O_8 over 15 m with a maximum 13.6 wt. % U_3O_8 over 0.5 m; Aubin, 2011), whose location along the regional unconformity between the basal Otish Supergroup sediments and the underlying metamorphosed Archean volcano-sedimentary rocks (Fig. 1) is consistent with unconformity-related uranium systems (Gatzweiler, 1987; Beyer et al., 2012). New geochronological and geochemical data, summarized in this report, provide additional constraints on the timing of formation and evolution of the Otish basin, whereas revised mineral parageneses, whole-rock geochemistry and mineral chemistry of the hydrothermally-altered rocks that host the uranium minerals at the Camie River prospect establish the spatial and temporal relationships between alteration and uranium mineralization.

Geological Background

The Otish Basin is located at the southeastern margin of the Archean Superior Province, just north of the Grenville Tectonic Front (Fig. 1). The 150 by 50 km basin is host to the Otish Supergroup, a ca.1500 m thick, predominantly clastic, sedimentary sequence composed of conglomerate and sandstone of the Indicator Group, and sandstone, argillaceous sandstone, minor conglomerate and dolostone of the conformably overlying Peribonca Group (Chown and Caty, 1973; Gatzweiler, 1987; Genest, 1989; Beyer et al., 2012). The Otish Supergroup unconformably overlies an Archean basement, which consists of high-grade metamorphic (Epervanche Complex) and volcano-sedimentary (Tichegami Group) rocks, cut by younger felsic intrusions. The Archean basement is intruded by the northwest-trending Mistassini

Milidragovic, D., Lesbros-Piat-Desvial, M., King, J.J., Beaudoin, G., Hamilton, M.A., and Creaser, R.A., 2015. The Otish Basin: basin evolution and formation of the Camie River uranium deposit, Quebec, *in* Targeted Geoscience Initiative 4: unconformity-related uranium systems, (ed.) E.G. Potter and D.M. Wright; Geological Survey of Canada, Open File 7791, p. 115–122. doi:10.4095/295776

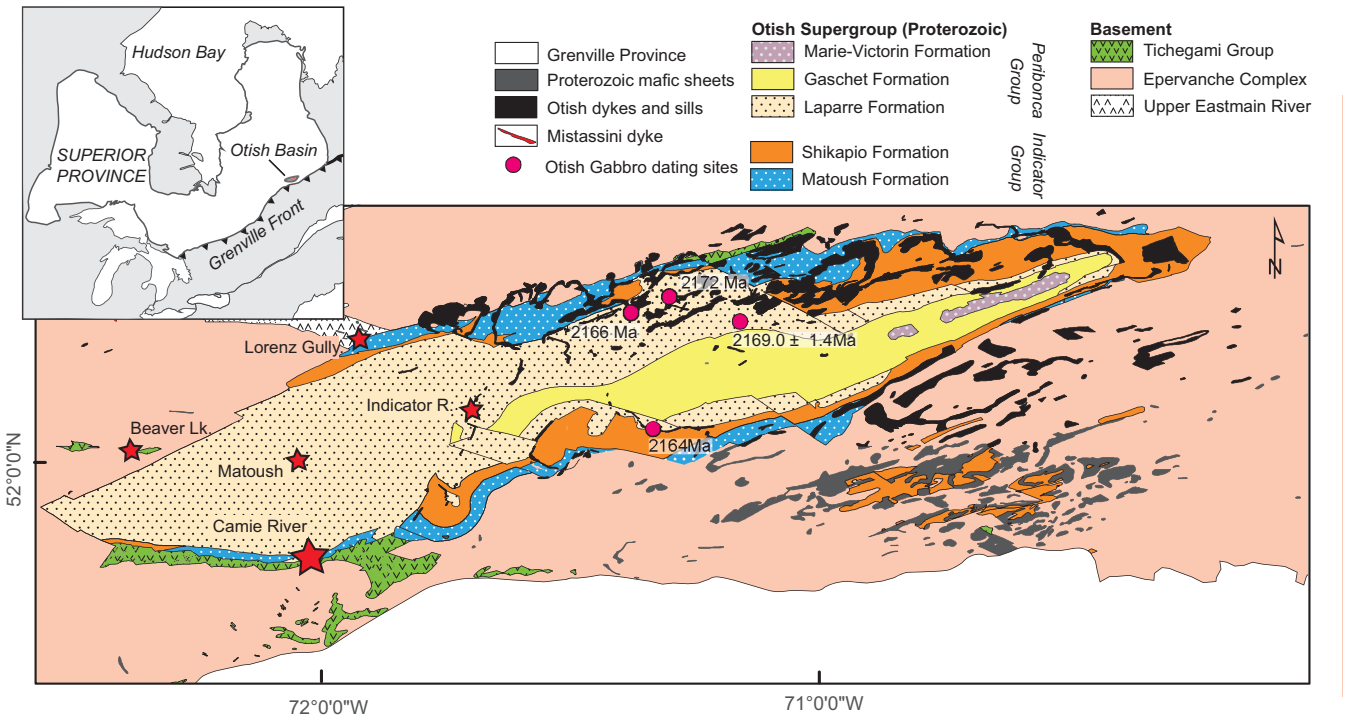

Figure 1. Geological map of the Otish Basin (modified from Lesbros-Piat-Desvial, 2014), showing select uranium showings (stars). Inset: location of Otish Basin in relation to the Superior Province.

dyke swarm, dated at 2515 ± 3 Ma (U-Pb baddeleyite; Hamilton, 2009). As the Mistassini dykes do not intrude the overlying Otish Basin sedimentary rocks, their age defines the maximum age of the Otish Supergroup.

The Otish Supergroup was intruded by dykes and sills of the Otish Gabbro suite (Fahrig and Chown, 1973; Chown and Archambault, 1987). Based on K-Ar results (1465 Ma; Wanless et al., 1965) and Sm-Nd age determinations (1730 ± 10 Ma and 1710 ± 30; C. Brooks in Ruhlmann et al., 1986; Gatzweiler, 1987; Höhndorf et al., 1987), the Otish Gabbros were long thought to have been emplaced during the period 1750–1710 Ma. This estimate is significantly younger than the more recent U-Pb baddeleyite age of 2169 ± 1.4 Ma for an upper Otish Gabbro sill presented by Hamilton and Buchan (2007). Late Paleoproterozoic U-Pb ages, indistinguishable from the ca. 1730 Ma Sm-Nd age reported by Gatzweiler (1987) and Höhndorf et al. (1987), have also been obtained from uraninite at the Camie River (1723 ± 16 Ma; Höhndorf et al., 1987; 1721 ± 20 Ma; Beyer et al., 2012) and Lorenz Gully (1717 ± 20 Ma; Höhndorf et al., 1987) prospects. The latter age coincidence led Beyer et al. (2012) to propose that the intrusion of the Otish Gabbros promoted the circulation of U-rich basinal brines that resulted in formation of the Camie River deposit.

During the Mesoproterozoic Grenville Orogeny (ca. 1.09–0.98 Ga; Hynes and Rivers, 2010), the Otish Basin and proximal basement rocks developed both dextral and sinistral strike-slip faults. The northwestern part of the basin underwent brittle deformation and sub-greenschist facies metamorphism limited to fault zones, whereas the southeastern part of the basin experienced ductile deformation and increasing regional metamorphic grade from greenschist to amphibolite facies close to the Grenville Front (Chown, 1979; 1984).

Geology of the Camie River prospect

Uranium mineralization at the Camie River prospect is dominated by uraninite, variably altered to brannerite and coffinite (Ruzicka and LeCheminant, 1984; Gatzweiler, 1987; Höhndorf et al., 1987; Beyer et al., 2012). According to Gatzweiler (1987), Beyer et al. (2012), and Lesbros-Piat-Desvial (2014), the high-grade mineralization is mainly hosted by sub-vertical graphitic schists ± massive sulphides that coincide with reverse faults that offset the unconformity between the Otish Supergroup (Matoush Formation) and the underlying Archean Hippocampe Belt (Tichegami Group). Mineralization is also hosted by faulted fluviatile sandstones and conglomerates of the Matoush Formation, near basement wedges (Lesbros-Piat-Desvial, 2014). As reported by Gatzweiler (1987) and Höhndorf et al. (1987), the uranium mineralization is polymetallic with enrichments in Mo, Cu, Co, Ni, As, Se, Nb, V, Ag and Au (± Th) that coincide with a zoned, mushroom-shaped alteration halo composed of an inner Fe-Mg chlorite and Fe-dolomite zone, and an outer albite, chlorite and pyrite zone.

Mineral paragenesis of the basement rocks at the Camie River prospect

The study of the Camie River prospect is based on the description of samples from 15 mineralized (n =6) and non-mineralized (n =9) diamond drill-holes. Sample details, such as the locations of the drill-holes and depths from which the

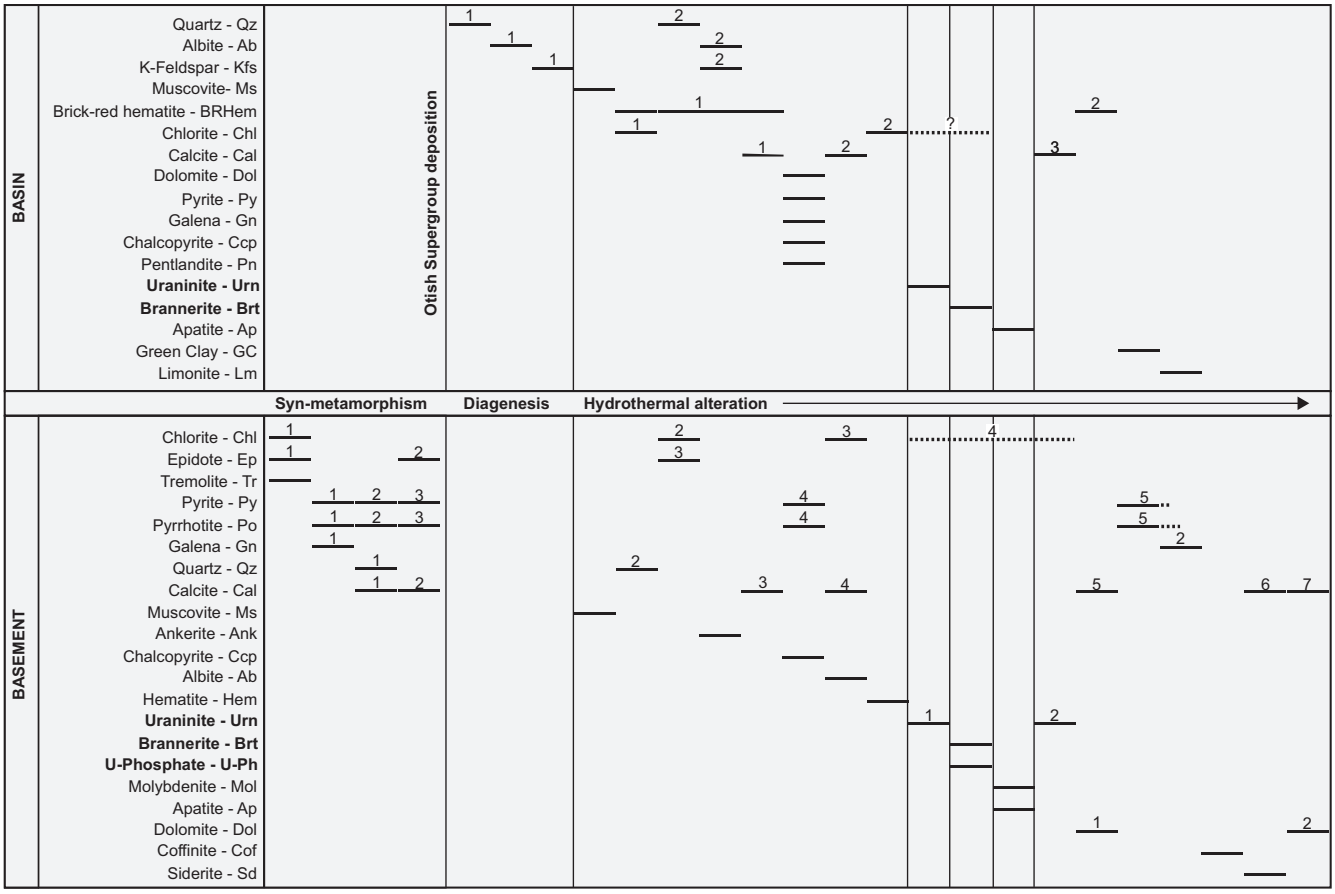

Figure 2. Paragenetic sequence of minerals associated with metamorphism, diagenesis and hydrothermal alteration at the Camie River prospect. Numbers indicate the different generations of a mineral. Vertical lines into basin and basement paragenesis indicate hydrothermal alteration and mineralization events which are recognized to have synchronously affected both sedimentary and basement rocks (Lesbros-Piat-Desvial, 2014).

samples were obtained, are presented in Lesbros-Piat-Desvial (2014). At the Camie River prospect, basement (Tichegami Group) and basin sedimentary rocks (Otish Supergroup) have been affected by several stages of hydrothermal alteration and are cut by several types of veins (Beyer et al., 2012; Lesbros-Piat-Desvial, 2014; Fig. 2). The basement rocks are moderately to strongly chloritized (*Chl1*) and contain coarse-grained pyrite (*Py1*), pyrrhotite (*Po1*), and minor galena (*Gn1*). The basement rocks are cut by numerous, centimeter-scale, quartz (*Qz1*) and calcite (*Cal1*) veins parallel to foliation, which contain disseminated pyrite (*Py2*) and pyrrhotite (*Po2*). The *Qz1* quartz and *Cal1* calcite veins are cut by later calcite (*Cal2*) and/or epidote (*Ep2*) veins that contain minor disseminated pyrite (*Py3*) and pyrrhotite (*Po3*).

After basement erosion and deposition of Otish Supergroup, pervasive coarse- to fine-grained muscovite alteration affected the top of the Tichegami Group down to several meters where the altered basement rocks appear bleached. The muscovite-altered basement rocks are cut by quartz veins (*Qz2*), followed by chlorite and epidote veins (*Chl2 and Ep3*, respectively). *Chl2* chlorite and *Ep3* epidote veins are cut by rare ankerite veins, themselves cut by later calcite veins (*Cal3*). Pyrite (*Py4*), pyrrhotite (*Po4*) and minor chalcopyrite fill fractures in previous *Cal3* calcite and *Ep3* epidote veins.

In basement rocks, uranium mineralization comprises a first generation of disseminated Pb-rich uraninite (*Urn1*) that is replaced by brannerite low in Ce and Fe, but rich in U, Pb, Si and Nb. Brannerite contains abundant inclusions of *Urn1* uraninite and few inclusions of galena (*Gn1*). *Urn1* uraninite is also replaced by an unidentified uraniferous phosphate that contains rare *Gn1* galena inclusions. The uraniferous phosphate is replaced by rare apatite. Disseminated and euhedral *Urn1* uraninite (< 3 μm) is intergrown with molybdenite, forming irregular aggregates and veins. Fine-grained (< 10 μm), euhedral molybdenite crystals are commonly cemented by galena (*Gn2*). Molybdenite is moulded by a second generation of Pb-rich uraninite (*Urn2*).

The uranium mineralization is cut by carbonate veins (*Dol1* and *Cal5*; < 10 cm), which are only found in rocks containing uranium minerals. *Gn2* galena cements fractures in disseminated pyrite (*Py5*) and pyrrhotite (*Po5*) inside *Dol1* dolomite and *Cal5* calcite veins. In *Dol1* dolomite veins, late and minor coffinite replaces and fills fractures in *Po5* pyrrhotite and *Gn2* galena. Uranium minerals and molybdenite are also cut by small *Py5* pyrite and siderite veins. The latest mineral phases observed in basement rocks

are carbonate veins: calcite (*Cal6*) and siderite, and finally calcite (*Cal7*) and dolomite (*Dol2*).

Mineral paragenesis of the basin sedimentary rocks at the Camie River prospect

In the Otish Basin sedimentary rocks, early diagenetic quartz (*Qz1*) is rare and forms overgrowths on detrital quartz grains. It is almost completely replaced by orange/pink-coloured feldspathic cement composed of two feldspars: (1) early albite (*Ab1*) progressively replaced by (2) later potassic feldspar (*Kf1*). The early diagenetic quartz (*Qz1*) cement and the feldspathic (*Ab1* and *Kf1*) cement are replaced by the same coarse- to fine-grained green muscovite observed in the basement rocks. In basin sedimentary rocks, intergrown muscovite and illite form pore-filling aggregates of irregular, platy crystals or minute flakes. The feldspathic and muscovite alteration types appear to be the two principal types of pervasive hydrothermal modification of the sedimentary rocks, forming three zones of hydrothermal alteration from the bottom to the top of the stratigraphic sequence (lower, interdigitation and upper zones; Fig. 3). The muscovite alteration is cut by narrow (< 5 mm) chlorite veins (*Chl1*) associated with moderate brick-red hematite alteration (*BRHem1*), more commonly located near fracture zones. Rare quartz veins (*Qz2*; <10 cm) are associated with *BRHem1* brick-red hematite alteration, as well as paragenetically later albite (*Ab2*), K-feldspar (*Kfs2*) and calcite (*Cal1*) veins. However, the *BRHem1* brick-red hematite alteration often occurs isolated from other minor alteration and veins.

In the basin sedimentary rocks, uranium mineralization and fractured zones commonly contain narrow dolomite veins with disseminated, euhedral, pyrite, and with fractures cemented by galena with minor chalcopyrite and pentlandite. Dolomite in veins is partly replaced by calcite (*Cal2*). Fractured zones also contain a spatially associated chlorite alteration (*Chl2*). In uranium-mineralized basin sedimentary rocks, disseminated, Pb-rich uraninite (*Urn1)*, similar to that found in the basement rocks, is progressively replaced by Nb-rich brannerite that is itself replaced by rare apatite.

The uranium mineralization is cut by small calcite veins (*Cal3*), which are themselves cut by brick-red hematite veins (*BRHem2*). The brick-red hematite veins (*BRHem2*) are cut by later green clay veins. In the basin sedimentary rocks, the paragenetic sequence ends with limonite in veins and limonite alteration. Limonite weathers the Otish Supergroup rocks over several meters below the current erosion surface, and infiltrates deeper in fractured zones.

Lithogeochemistry of the Camie River prospect

Forty-one non-mineralized (15 feldspathic and 26 muscovite-altered) sandstone and conglomeratic sandstone samples from fourteen diamond drill-holes at the Camie River prospect, in addition to nine (5 muscovite and 4 "least-altered") sandstone and conglomeratic sandstone samples from a diamond drill-hole (OTS-01) ~18 km NW of the Camie River prospect, were analyzed for major and trace elements.

The least-altered sandstones from OTS-01 and feldspathic sandstones from Camie River have relatively low Al_2O_3 and K_2O, but higher SiO_2 contents, compared to the muscovite-altered sandstones. The feldspathic sandstones at the Camie River prospect are characterized by the lowest LOI values (≤0.5 wt. %) and highest Na_2O concentrations. Notably, Na_2O concentrations in the feldspathic sandstones increase from 1.0 wt. %, 125 m above the unconformity, to 3.4 wt. % at the unconformity and near the uranium mineralization (Fig. 4). In contrast, the least-altered and muscovite-altered sandstones have relatively high LOI values (≥ 1 wt. %) and uniformly low Na_2O contents (<0.5 wt. %).

In order to characterize feldspathic and muscovite alteration at the Camie River prospect, the Grant (1986) isocon method was applied using the average of three lithochemically similar "least-altered" sandstones from the diamond drill hole OTS-01. Relative to the "least-altered" sandstones,

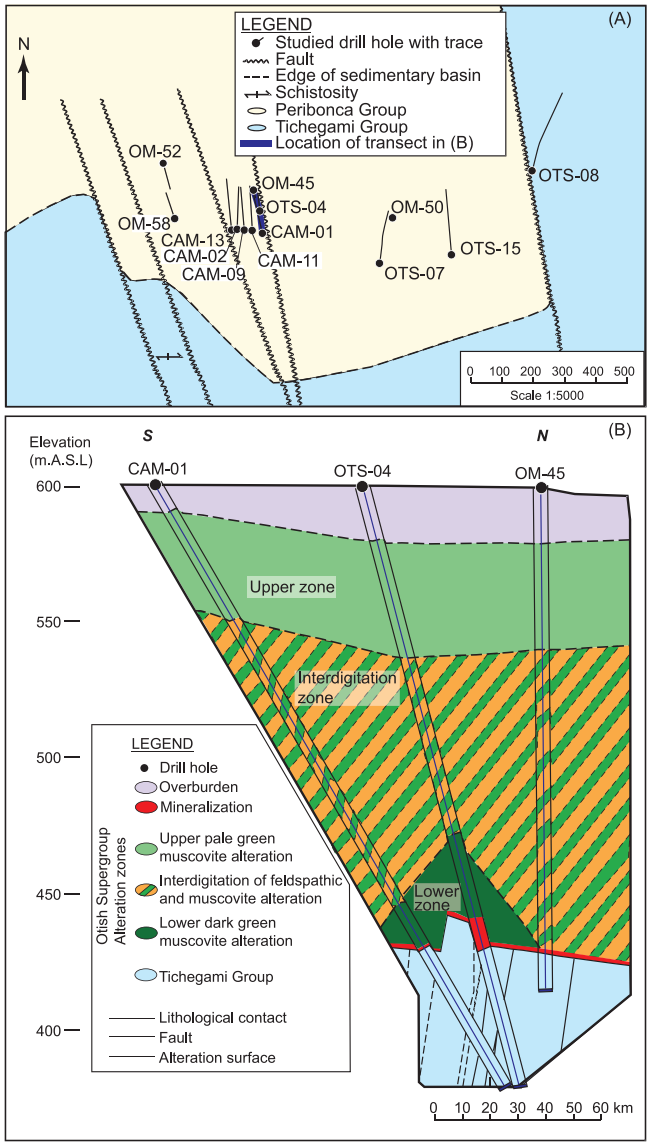

Figure 3. (A) Map of the Camie River prospect, showing the locations of 14 out of 15 drill-holes, sampled as part of this study (modified from Aubin, 2011). **(B)** Schematic cross-section, showing the distribution of the principal types of alteration (feldspathic and muscovite) in the sedimentary rocks of the Camie River prospect, from Lesbros-Piat-Desvial (2014).

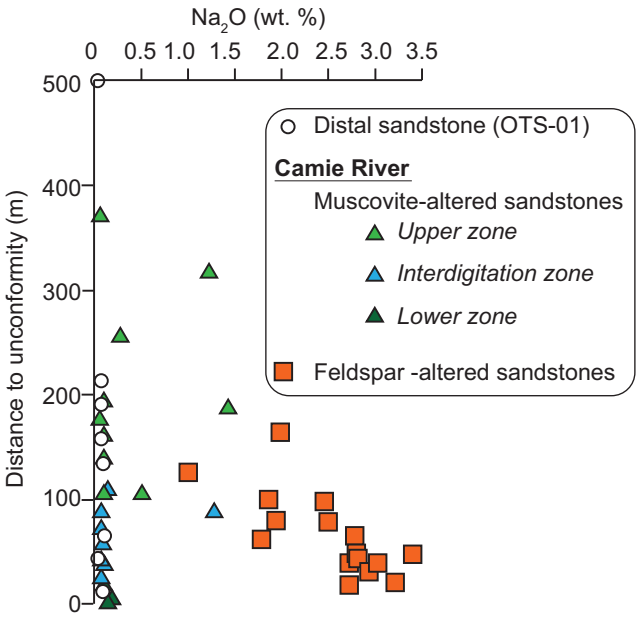

Figure 4. Na_2O concentrations (wt. %) in the sandstones from Camie River and OTS-01 versus distance to the unconformity (modified from Lesbros-Piat-Desvial, 2014).

the non-mineralized, altered sandstones from Camie River and OTS-01 are enriched in the heavy rare earth elements (HREE) and yttrium. The well-defined linear array of HREE (+Y) in the isocon plots, suggests the immobility of these elements during alteration and diagenesis. Applying the isocon method suggests that the altered sandstones experienced mass losses of at least 30% (Grant, 1986). This mass loss was likely accomplished through a combined increase in porosity and decrease in rock density. The feldspathic sandstones at the Camie River prospect show a mass loss of about 75%, higher than muscovite-altered sandstones from the upper (about 30% mass loss) and interdigitation (about 40% mass loss) alteration zones, but close to that from the lower alteration zone (about 80%). The muscovite-altered sandstones from Camie River show an increasing mass loss with depth. In comparison, the muscovite-altered sandstones from OTS-01 show a mass loss of about 50%.

Age of molybdenite mineralization at Camie River prospect

Metal-free crushing followed by conventional magnetic and gravity separation techniques (c.f. Selby et al., 2003) were used to isolate molybdenite from the uraninite-bearing sample 8570 (U ~95,500 ppm, Mo ~13,700 ppm), which was collected from drill-hole CAM-11 (Fig. 3) at a depth of ~197 m. The mineralized sample is hosted within a graphitic metapelite of the Tichegami Group. Molybdenite is disseminated with a typical layered texture, and intergrown with *Urn1* uraninite (Fig. 5). Duplicate analyses of molybdenite at University of Alberta, using the methods described by Selby and Creaser (2004) and Markey et al. (2007), yield a Re-Os model age of 1724 ± 4.9 Ma (Lesbros-Piat-Desvial, 2014). The Re-Os model age is indistinguishable from the U-Pb uraninite (*Urn1*) ages of 1723 ± 16 Ma and 1721 ± 20 Ma

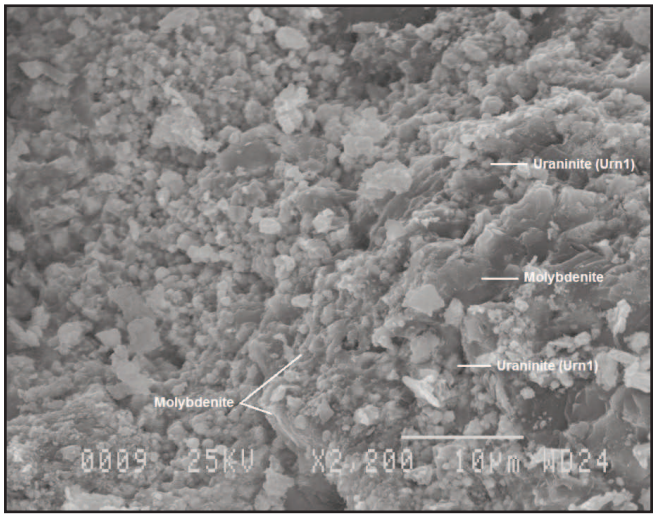

Figure 5. Secondary electron (SE) image of sample 85780, which contains 1724 ± 4.9 Ma molybdenite intergrown with uraninite.

reported by Höhndorf et al. (1987) and Beyer et al. (2012), respectively.

Age and evolution of the Otish Basin

Petrology and age of the Otish Gabbros

The Otish Gabbro dykes and sills, which intrude the Otish Basin, provide an important constraint on the age of the basin. Previous age determinations (Gatzweiler, 1987; Höhndorf et al., 1987; Hamilton and Buchan, 2007) suggest: 1) one or more episodes of gabbro emplacement with the ca. 1.73 Ga episode broadly coinciding with uranium mineralization in the western Otish Basin (Beyer et al., 2012), or 2) basin-wide thermal disturbance and resetting of the Sm-Nd isotopic system that accompanied hydrothermal activity and uranium mineralization.

The bulk of the exposed Otish Gabbro outcrops consist of three sills that dip shallowly (≤15°) to the south (Fig. 1). The sills, Novet (basal), Margat (middle), and Conflans (uppermost), terminate along northeast-trending dykes and are discontinuous throughout the Otish Basin (Fahrig and Chown, 1973; Chown and Archambault, 1987). The sills display rhythmic layering and cumulate textures, and range in thickness from <300 m to >500 m. The dykes have variable northeast to northwest strikes, and range in width from 30–200 m. Both dykes and sills are plagioclase and clinopyroxene-dominated, display variable grain size and textures, and are weakly to strongly altered. Ubiquitous saussuritized plagioclase and abundance of chlorite, epidote, actinolite, and sericite indicate greenschist-facies metamorphic conditions. Olivine was the earliest mineral to crystallize, as indicated by the presence of subhedral to resorbed olivine crystals, partially to fully enclosed by plagioclase and clinopyroxene.

The Otish Gabbros were subdivided into two geochemical groups based on differences in their major and incompatible trace element contents (Fig. 6). Samples belonging to both groups have been collected from the same sill, suggesting that the geochemical variations do not reflect multiple

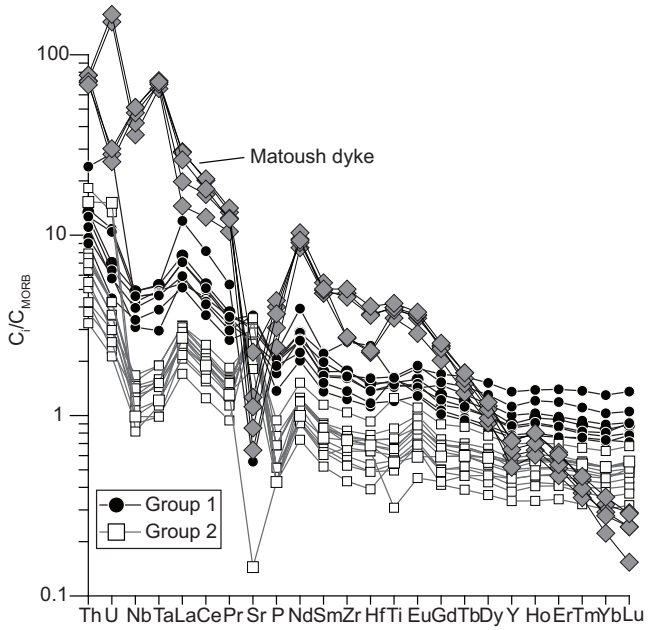

Figure 6. MORB-normalized (Sun and McDonough, 1989) trace element abundances of Otish Gabbro samples examined in this study, plotted by group. Also shown are the compositions of 5 least-altered samples of the subsurface Matoush dyke.

episodes of intrusion. Group 1 Otish Gabbros are characterized by SiO_2 (48–56 wt. %) contents that overlap, but are lower overall than those of the Group 2 gabbros (SiO_2 =50–53 wt. %). In contrast, FeO^{TOT} (11–16 wt. %) and TiO_2 (1.6–2.2 wt. %) have lower overall abundances in the Group 1 gabbros than in the Group 2 gabbros (FeO^{TOT} =8–15 wt. %, TiO_2 =0.4–1.6 wt. %). The most striking difference between the two groups is their trace element profiles. Group 1 gabbro samples are characterized by higher absolute abundances of all incompatible trace elements, except for Sr, than Group 2 samples (Fig. 6). The geochemical differences between the Group 1 and Group 2 Otish gabbros are ascribed to the effects of crystal accumulation (Milidragovic et al., 2014). Mass-balance modelling of trace elements suggests that the Group 2 gabbros are crystal cumulates formed by physical addition of plagioclase and clinopyroxene to Group 1 gabbros, which may approximate liquid compositions.

Samples dated at the University of Toronto as a part of this study include both Group 1 and Group 2 compositions, the locations of which are shown on Figure 1. Baddeleyite crystals from the Novet (Group 1) and Margat (Group 2) sills yield isotope dilution - thermal ionization mass spectrometry (ID-TIMS) U-Pb crystallization ages of 2172 and 2166 Ma, respectively, consistent with a previous determination on the uppermost (Conflans) sill at 2169.0 ± 1.4 Ma (Hamilton and Buchan, 2007; *submitted*). Another Otish Gabbro sample, representing an irregular satellite dyke in the south-central part of the basin has yielded an emplacement age of 2164 Ma, based on U-Pb baddeleyite dating. The geochemical and geochronological constraints from the Otish Gabbro dykes and sills indicate that they were emplaced as a result of a principal magmatic pulse ca. 2165–2170 Ma. Furthermore, these results constrain the age of the Otish Basin deposition to ca. 2515–2165 Ma and suggest that uranium mineralization postdates the basin formation by >450 million years.

The Matoush Dyke

At the Matoush deposit, uranium mineralization is spatially associated with the subsurface Matoush dyke, a 0.5–3.0 m wide intrusion that follows the northeast-striking Matoush Fault, northeast of the Camie River deposit (Fig. 1; Alexandre et al., 2014). The least-altered samples from the Matoush dyke are characterized by a fine-grained, biotite-phyric texture. Rare large (>0.5 mm) polygonal crystals, composed of calcite-dolomite cores and rims of serpentine, have prismatic grain terminations and display "tracks" of fine-grained magnetite, suggesting they may be pseudomorphs after olivine. The groundmass of the least-altered samples of the Matoush dyke is dominated by serpentine and carbonate, with the more altered samples containing increased carbonate contents.

The strongly fractionated trace element profile of the Matoush dyke samples reflects both a strong enrichment in LREE and depletion in HREE relative to MORB (Fig. 6). Furthermore, in contrast to the Otish Gabbros, the Matoush dyke shows an enrichment in HFSE relative to similarly compatible REE. The strongly fractionated REE profiles, the highly enriched LREE, and elevated concentrations of the HFSE suggest an alkaline affinity for the Matoush dyke, and resemble ultramafic lamprophyres and kimberlites (Rock, 1991; Tappe et al., 2004).

Geophysical imaging (J. Lafontaine, pers. comm.) suggests that the Matoush dyke cross-cuts an Otish Gabbro dyke and is therefore likely ≤2170 Ma. Given this relationship, it is possible that intrusion of Matoush-related magmas promoted circulation of uranium-rich brines and precipitation of uranium-minerals, as previously suggested for the Otish Gabbro by Beyer et al. (2012). Efforts to date the crystallization age of the Matoush dyke directly via U-Pb methods are in progress.

Implications for uranium exploration

The temporal relationship between the uranium mineralization in the Otish Basin and the host rocks differs from other major sedimentary basin-hosted Proterozoic uranium districts. The U-Pb and Re-Os ages of uraninite and molybdenite at the Camie River deposit postdate the minimum age of the Otish Basin by ≥450 m.y., significantly exceeding the characteristic time-gap of other major uranium mineralization events in the Proterozoic. For instance, the primary ca. 1590 Ma uranium mineralization in the Athabasca Basin (Alexandre et al., 2009) occurred approximately 150 m.y. after the formation of the basin (ca. 1740 Ma; Orell et al., 1999; Rainbird et al., 2007), and even overlaps deposition of the uppermost units (1541 ± 13 Ma; Creaser and Stasiuk, 2007). Similarly, the ca. 1680 Ma age of mineralization at the Jabiluka uranium deposit was synchronous with diagenesis of the basin-filling Kombolgie Subgroup following basin formation at ca. 1822 Ma (Sweet et al., 1999; Polito et al., 2005; 2011). These observations make the uranium mineralization of the Otish Basin unique and highlight the neces-

sity for better understanding of the basin's post-digenetic tectonothermal history, namely ca. 1.72 Ga. Hydrothermal activity of similar age (ca. 1.7 Ga) has also resulted in the polymetallic vein mineralization (including U) in the ca. 2.45–2.22 Ga Huronian Supergroup in the southern Superior Province (Potter and Taylor, 2010 and references therein). The hydrothermal activity included both regional K- (1728–1688 Ma; Fedo et al., 1997) and Na- (1700 ±2 Ma; Schandl et al., 1994) metasomatism, and the emplacement of the polymetallic calcite-quartz veins (ca. 1675 Ma; Potter & Taylor, 2009). Fedo et al., (1997) and Potter and Taylor (2010) ascribed the ca. 1.7 Ga hydrothermal activity to the waning stages of the Penokean Orogeny. Establishing the age of the Matoush dyke, thus, appears to be critical to understanding the sequence of geological events that led to uranium mineralization in the Otish basin, and to evaluating the regional extent of ca. 1.7 Ga hydrothermal activity along the southern margin of the Superior Province.

Conclusions

1. This report demonstrates that the age of the Otish Basin is older than previously thought. The maximum age of the Otish Basin is defined by the age of the unconformably underlying ca. 2515 Ma Mistassini dyke swarm (Hamilton, 2009). The minimum age of the basin corresponds to the emplacement age of the Otish Gabbro suite (ca. 2170 Ma). The younger (ca. 1730 Ma) Sm-Nd isotopic age of the Otish Gabbro suite is ascribed to later isotopic resetting and LREE remobilization.
2. A younger igneous event, which followed the emplacement of the Otish Gabbros, is inferred based on the mineralogy and geochemistry of the subsurface Matoush dyke. The Matoush dyke has lamprophyric affinity.
3. Re-Os dating of molybdenite intergrown with uraninite (*Urn1*) confirms the previous interpretations of the age of the main uranium mineralization event ca. 1720 Ma, which postdates the formation of the Otish basin by ≥ 450 M.y.
4. Uranium + Mo + Cu + Co + Ni + As + Se + Nb + V + Ag + Au ± Th mineralization at the Camie River prospect postdates the early and peak diagenetic Na- and K- feldspathic and muscovite alteration of the basin sedimentary rocks, and is focussed along the unconformable contact between the Paleoproterozoic Otish Supergroup (Matoush Formation) and the Archean Basement. Sandstones proximal to the unconformable contact and uranium mineralization show elevated Na_2O concentrations (> 1 wt. %)

Acknowledgments

Funding for this research was provided by contributions from Cameco Corporation and a grant to G. Beaudoin through the Targeted Geoscience Initiative 4 (TGI-4) uranium ore systems project of Natural Resources Canada. Constructive peer-reviews by S. Beyer and E.G. Potter improved the quality of the manuscript.

References

Alexandre, P., Kyser, K., Thomas, D., Polito, P., and Marlat, J., 2009. Geochronology of unconformity-related uranium deposits in the Athabasca Basin, Saskatchewan, Canada and their integration in the evolution of the basin; Mineralium Deposita, v. 44, 41–59.

Alexandre, P., Peterson, R.C., Kyser, K., Layton-Matthews, D., and Joy, B., 2014. High-Cr minerals from the Matoush Uranium deposit in the Otish Basin, Quebec, Canada; The Canadian Mineralogist, v. 52, p. 61–75.

Aubin, A., 2011. The Camie-Beaver and Otish South projects and the uranium potential of the Otish sedimentary basin; Symposium Mines Baie-James, May 31, 2011, Abstracts, p.10.

Beyer, S.R., Kyser, K., Hiatt, E.E., Polito, P.A., Alexandre, P., and Hoksbergen, K., 2012. Basin evolution and unconformity-related Uranium mineralization: The Camie River U prospect, Paleoproterozic Otish Basin, Quebec; Economic Geology, v. 107, p. 401–425.

Chown, E.H., 1979. Structure and metamorphism of the Otish Mountain area of the Grenvillian Foreland Zone, Québec: summary; Geological Society of America Bulletin, v. 90, p. 13–15.

Chown, E.H., 1984. Mineralization Controls in the Aphebian formations, Chibougamau; Mistassini and Otish areas; Canadian Institute of Mining and Metallurgy, Special Volume 34, p. 229–243.

Chown, E.H. and Archambault, G., 1987. The transition from dyke to sill in the Otish Mountains, Quebec; relations to host-rock characteristics; Canadian Journal of Earth Sciences, v. 24, p. 110–116.

Chown, E.H. and Caty, J.L., 1973. Stratigraphy, petrography, and paleocurrent analysis of the Aphebian clastic formations of the Mistassini-Otish Basin; Geological Association of Canada, Special Paper 12, p. 49–71.

Creaser, R.A. and Stasiuk, L.D., 2007. Depositional age of the Douglas Formation, northern Saskatchewan, determined by Re-Os geochronology; in EXTECH IV: geology and uranium EXploration TECHnology of the Proterozoic Athabasca Basin, Saskatchewan and Alberta, (ed.) C.W. Jefferson and G. Delaney; Geological Survey of Canada Bulletin, v. 588, p. 341–346.

Fahrig, W.F. and Chown, E.H., 1973. The Paleomagnetism of the Otish gabbro from north of the Grenville Front, Quebec; Canadian Journal of Earth Sciences, v. 10, p. 1556–1564.

Fedo, C.M, Young, G.M, Nesbitt, H.W. and Hanchar, J.M., 1997. Potassic and sodic metasomatism in the Southern Province of the Canadian Shield: evidence from the Paleoproterozoic Serpent Formation, Huronian Supergroup, Canada; Precambrian Research, v. 84, p. 17–36.

Gatzweiler, R., 1987. Uranium mineralization in the Proterozoic Otish Basin, central Quebec, Canada; Berlin-Stuttgart, Gebrüder Borntraeger, Monograph Series on Mineral Deposits 27, p. 27–48.

Genest, S., 1989. Histoire géologique du Bassin d'Otish, Protérozoïque Inférieur (Québec); Ph.D. thesis, Université De Montréal, Montréal, Québec, 329 p.

Grant, J.A., 1986. The isocon diagram - a simple solution to Gresens' equation for metasomatic alteration; Economic Geology, v. 81, p. 1976–1982.

Hamilton, M.A., 2009. Datation isotopique (U-Pb) d'un diabase de l'essaim de dykes Mistassini, Québec - U-Pb isotopic dating of a diabase dyke of the Mistassini swarm, Québec; Ministère des Ressources Naturelles et de la Faune, Québec, GM 65972, 13 p.

Hamilton, M.A. and Buchan, K.L., 2007. U-Pb baddeleyite age for Otish Gabbro: Implications for correlation of Proterozoic sedimentary sequences and magmatic events in the eastern Superior Province; Joint Annual Meeting of the Geological Association of Canada – Mineralogical Association of Canada, Abstracts, v. 32, p. 35.

Hamilton, M.A. and Buchan, K.L., *submitted*. A 2169 Ma U-Pb baddeleyite age for the Otish Gabbro, Quebec: Implications for correlation of Proterozoic magmatic events and sedimentary sequences in the eastern Superior Province; Submitted to Canadian Journal of Earth Sciences, Nov. 2014.

Höhndorf, A., Bianconi, F., and Von Pechmann, E., 1987. Geochronology and metallogeny of vein-type uranium occurrences in the Otish Basin area, Quebec, Canada; in Metallogenesis of Uranium Deposits: Proceedings of a Technical Committee Meeting on Metallogenesis of Uranium Deposits, Vienna, IAEA, p. 233–260.

Hynes, A.J. and Rivers, T., 2010. Protracted continental collision – evidence from the Grenville Orogen; Canadian Journal of Earth Sciences, v. 47, p. 591–620.

Lesbros-Piat-Desvial, M., 2014. Hydrothermal alteration and uranium min-

eralization at the Camie River prospect (Otish Basin, Québec); M.Sc. thesis, Université Laval, Québec City, Québec, 130 p.

Markey, R.J, Stein, H.J, Hannah, J.L., Selby, D. and Creaser, R.A., 2007. Standardizing Re-Os geochronology: a new molybdenite reference material (Henderson, USA) and the stoichiometry of Os salts; Chemical Geology, v. 244, p. 74–87.

Milidragovic, D., King, J.J., Beaudoin, G., and Hamilton, M.A., 2014. Petrology and geochemistry of the Otish Gabbros and comparison to ca. 2.17 Ga mafic dyke swarms of the Superior Province; Joint Annual meeting of the Geological Association of Canada – Mineralogical Association of Canada, Abstracts v.37, p.188-189.

Orrell, S.E., Bickford, M.E. and Lewry, J.F., 1999. Crustal evolution and age of thermotectonic reworking in the western hinterland of Trans-Hudson orogen, northern Saskatchewan; Precambrian Research, v. 95, p. 187–223.

Polito, P.A., Kyser, T.K., Thomas, D., Marlatt, J., and Drever, G., 2005. Re-evaluation of the petrogenesis of the Poterozoic Jabiluka unconformity-related uranium deposit, Northern Territory, Australia; Mineralium Deposita, v. 40, p. 257–288.

Polito, P.A., Kyser, T.K., Alexandre, P., Hiatt, E.E. and Stanley, C.R., 2011. Advances in understanding the Kombolgie Subgroup and unconformity-related uranium deposits in the Alligator Rivers Uranium Field and how to explore for them using lithogeochemical principles; Australian Journal of Earth Sciences, v. 58, p. 453–474.

Potter, E.G. and Taylor, R.P., 2009. The lead isotope composition of ore minerals from precious metal-bearing, polymetallic vein systems in the Cobalt Embayment, Northern Ontario: metallogenic implications; Economic Geology, v. 104, p. 869–879.

Potter, E.G. and Taylor, R.P., 2010. The stable and radiogenic isotopic atributes of precious-metal-bearing polymetallic veins from the Cobalt Embayment, Northern Ontario, Canada: genetic and exploration implications; The Canadian Mineralogist, v. 48, p. 391–414.

Rainbird, R.H., Stern, R.A., Rayner, N., and Jefferson, C.W., 2007. Age, provenance, and regional correlation of the Athabasca Group, Saskatchewan and Alberta, constrained by igneous and detrital zircon geochronology; in EXTECH IV: geology and uranium EXploration TECHnology of the Proterozoic Athabasca Basin, Saskatchewan and Alberta, (ed.) C.W. Jefferson and G. Delaney; Geological Survey of Canada Bulletin, v. 588, p. 193–210.

Rock, N.M.S., 1991. Lamprophyres; Blackie & Son, Glasgow, 285 pp.

Ruhlmann, F., Raynal, M., and Lavoie, S., 1986. Un exemple de métasomatisme alcalin albite-uranium dans le basin des Monts Otish, Québec; Canadian Journal of Earth Sciences, v. 23, p. 1742–1752.

Ruzicka, V. and LeCheminant, G.M., 1984. Uranium deposit research; in: Current Research, Part A, Geological Survey of Canada, Paper 84-1A, p. 39–51.

Schandl, E.S, Gorton, M.P. and Davis, D.W., 1994. Albitization at 1700 ±2 Ma in the Sudbury-Wanapitei Lake area, Ontario: implications for deep-seated alkalin magmatism in the Southern Province; Canadian Journal of Earth Sciences, v. 31, p. 597–607.

Selby, D. and Creaser, R.A., 2004. Macroscale NTIMS and microscale LA-MC-ICP-MS Re-Os isotopic analysis of molybdenite: Testing spatial restrictions for relaible Re-Os age determinations, and implications for the decoupling of Re and Os within Molybdenite; Geochimica et Cosmochimica Acta, v. 68, p. 3897–3908.

Selby, D., Creaser, R.A, Heaman, L.M. and Hart, C.J.R., 2003. Re-Os and U-Pb geochronology of the Clear Creek, Dublin Gulch, and Mactung deposits, Tombstone Gold Belt, Yukon, Canada: absolute timng relationships between plutonism and mineralization; Canadian Journal of Earth Sciences, v. 40, p. 1839–1852.

Sun, S. and McDonough, W.F., 1989. Chemical and isotopic systematics of oceanic basalts: implications for mantle composition and processes; in Magmatism in the ocean basins, (ed.) A.D. Saunders and M. Norry; Geological Society of London Special Publication 42, p. 313–345.

Sweet, I.P., Brakel, A.T. and Carson, L., 1999. The Kombolgie Subgroup - a new look at an old 'formation'; AGSO Research Newsletter, v. 30, p. 26–28

Tappe, S., Jenner, G.A., Foley, S.F., Heaman, L., Besserer, D., Kjarsgaard, B.A., and Ryan, B., 2004. Torngat ultramafic lamprophyres and their relation to the North Atlantic Alkaline Province; Lithos, v. 76, 491–518.

Wanless R K, Stevens, R.D., Lachance, G.R., and Rimsaite, R.Y.H., 1965. Age determinations and geological studies, Part I: Isotope ages; Geological Survey of Canada, Report 5, Paper 64-17, pt. 1, 126 p.

GEOLOGICAL SURVEY OF CANADA
OPEN FILE 7791

Targeted Geoscience Initiative 4: unconformity-related uranium systems

E.G. Potter[1] and D.M. Wright[2] (ed.)

[1] Geological Survey of Canada, 601 Booth Street, Ottawa, Ontario
[2] Peridot Geoscience Ltd., 19 Rein Terrace, Kanata, Ontario

2015

doi:10.4095/295776

This publication is available for free download through GEOSCAN (http://geoscan.nrcan.gc.ca/).

Recommended citation
Potter, E.G., and Wright, D.M. (ed.), 2015. Targeted Geoscience Initiative 4: unconformity-related uranium systems; Geological Survey of Canada, Open File 7791, 126 p. doi:10.4095/295776

Publications in this series have not been edited; they are released as submitted by the author.